

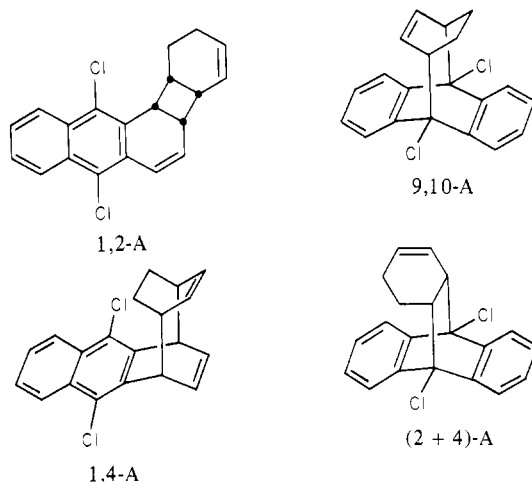
# Adiabatic S<sub>1</sub> 9,10-Dichloroanthracene Formation from Electronically Excited 9,10-Dichloroanthracene/1,3-Cyclohexadiene Photoadducts<sup>1</sup>

William K. Smothers and Jack Saltiel\*

Contribution from the Department of Chemistry, Florida State University, Tallahassee, Florida 32306. Received July 12, 1982

**Abstract:** The photochemistry and fluorescence of the two major photoadducts of 9,10-dichloroanthracene (DCA) and 1,3-cyclohexadiene (CHD) are described. The 1,2-adduct, 1,2-A ( $[2\pi_s + 2\pi_s]$  to the 1,2-positions of DCA), gives DCA and CHD as main photoproducts in several solvents,  $\phi_{1,2-A} \approx \phi_{DCA} \approx \phi_{CHD} \approx 0.3$ . It exhibits fluorescence characteristic of the naphthalene moiety (350–435 nm) and, in addition, gives DCA fluorescence (390–560 nm). The pronounced oxygen quenching effect of the latter shows that cleavage of singlet excited 1,2-A,  $^11,2-A^*$ , is in part adiabatic,  $\phi_{DCA}^{1,2-A^*} \approx 0.007$ –0.015. The 9,10-adduct, 9,10-A ( $[4\pi_s + 4\pi_s]$  to the 9,10-position of DCA), is efficiently destroyed by light,  $\phi_{9,10-A} \approx 1.0$ , but gives several products in addition to DCA and CHD,  $\phi_{DCA} \approx \phi_{CHD} \approx 0.11$ . Its fluorescence is identical with DCA fluorescence, corresponding to  $\phi_{DCA}^{9,10-A^*} \approx 0.0041$ –0.0068, depending on the solvent. The observations are discussed by using the current theoretical model for electrocyclic photochemical reactions. They suggest that if pericyclic minima are involved in adduct photocleavage and formation, they are isolated in the potential energy surface and do not readily interconvert.

Photocycloaddition of 9,10-dichloroanthracene (DCA) to 1,3-cyclohexadiene (CHD) yields three major adducts corresponding to allowed  $[2\pi_s + 2\pi_s]$  addition of CHD to the 1,2-positions of DCA (1,2-adduct) and  $[4\pi_s + 4\pi_s]$  additions of CHD to the 9,10- and



1,4-positions of DCA (9,10- and 1,4-adducts).<sup>2,3</sup> A reversibly formed nonfluorescing singlet exciplex,  $^1(DCA \cdot CHD)^*$ , is probably a common intermediate in these reactions.<sup>3</sup> The mechanism for the formation of a minor (<1%) forbidden  $[2\pi_s + 4\pi_s]$  adduct  $[(2 + 4)$ -adduct] has not been elucidated.<sup>3</sup>

Photochemically allowed concerted cycloadditions are characterized by correlation between the singly excited (S) states of addends and adduct, correlation of the doubly excited (D) state of addends with the ground (G) state adduct, and correlation of ground-state addends with doubly excited adduct (Figure 1).<sup>4</sup>

Intended, but avoided, crossing of the D and G states creates a pericyclic minimum on the excited electronic surface at the biradicaloid geometry where new bonds are partly formed and old bonds partly broken.<sup>4</sup> At larger intermolecular separation the exciplex energy minimum on S provides a reservoir of addends potentially ready for cycloaddition. If reaction is initiated by electronic excitation of the adduct, leakage from the pericyclic minimum and adiabatic<sup>5</sup> conversion along the S surface are energetically feasible pathways to electronically excited products, exciplex, and/or addends. Decay through the "funnel" or "hole" at pericyclic minima provides diabatic reaction paths to ground-state addends and adducts.<sup>4</sup> Diabatic pathways usually predominate and adiabatic photocleavage reactions are generally inefficient.<sup>6,7</sup> Inspection of Figure 1 shows that the photophysical and photochemical properties of  $[2 + 2]$  and  $[4 + 4]$  cycloadducts may provide a useful approach for examining the theoretical pericyclic minima.<sup>8</sup>

An earlier failure to detect 1,2-A<sup>2</sup> was traced to its efficient photocleavage to DCA and CHD.<sup>3</sup> Those initial observations and current interest in adiabatic and diabatic photocleavage reactions prompted the following spectroscopic and photochemical study of the 1,2- and 9,10-adducts. The findings reveal significant adiabatic photoreaction channels in both cases and suggest that if pericyclic minima are involved in the diabatic pathways, they differ significantly for the two adducts and do not interconvert.

## Results

**Spectroscopic Measurements.** Fluorescence spectra, uncorrected for nonlinearity of instrumental response, obtained by 320-nm excitation of argon-purged and oxygen-saturated acetonitrile solutions of 1,2-A are shown in Figure 2. Maximum intensities of emission bands are at 365, 383, 405, 428, and 454 nm. Excitation at 254 or 340 nm, where DCA absorbs strongly, rather than at 320 nm, the  $\lambda_{max}$  of 1,2-A, sharply increases the intensity of the 405-, 428-, and 454-nm bands relative to that of the 365- and 383-nm bands. The excitation spectrum obtained by monitoring 383-nm emission is analogous to the UV spectrum of 1,2-A, whereas monitoring emission at 454 nm gives an excitation spectrum which resembles a combination of 1,2-A and DCA UV

(1) (a) Supported by National Science Foundation Grants CHE77-23852 and CHE80-26701. (b) Taken from the Ph.D. Dissertation of W. K. Smothers, Florida State University, 1981.

(2) Yang, N. C.; Srinivasachar, K.; Kim, B.; Libman, J. J. *Am. Chem. Soc.* **1975**, *97*, 5006. cf. also: Srinivasachar, K. Ph.D. Dissertation, University of Chicago, 1975, which describes the isolation of 1,2-A in acetonitrile but not in benzene.

(3) Smothers, W. K.; Meyer, M. C.; Saltiel, J. J. *Am. Chem. Soc.* **1983**, *105*, 545.

(4) (a) Michl, J. *Pure Appl. Chem.* **1975**, *41*, 507. (b) Michl, J. *Photochem. Photobiol.* **1977**, *25*, 141, and references cited therein. For early work see especially: Longuet-Higgins, H. C.; Abrahamson, E. W. *J. Am. Chem. Soc.* **1965**, *87*, 2045. Zimmerman, H. E. *J. Am. Chem. Soc.* **1966**, *88*, 1566. van der Lugt, W. Th. A. M.; Oosterhoff, L. J. *J. Am. Chem. Soc.* **1969**, *91*, 6042.

(5) Förster, Th. *Pure Appl. Chem.* **1970**, *24*, 433.

(6) For a review of adiabatic photoreactions, see: Turro, N. J.; McVey, J.; Ramamurthy, V.; Lechten, P. *Angew. Chem., Int. Ed. Engl.* **1979**, *18*, 572.

(7) For examples of very efficient adiabatic photocleavage, see: (a) Yang, N. C.; Chen, M.-J.; Chen, P.; Mak, K. T. *J. Am. Chem. Soc.* **1982**, *104*, 853.

(b) Becker, H.-D.; Sandros, K.; Andersson, K. *Chem. Phys. Lett.* **1981**, *77*, 246. (c) Okada, T.; Kida, K.; Mataga, N. *Chem. Phys. Lett.* **1982**, *88*, 157.

(8) Caldwell, R. A.; Creed, D. *Acc. Chem. Res.* **1980**, *13*, 45.

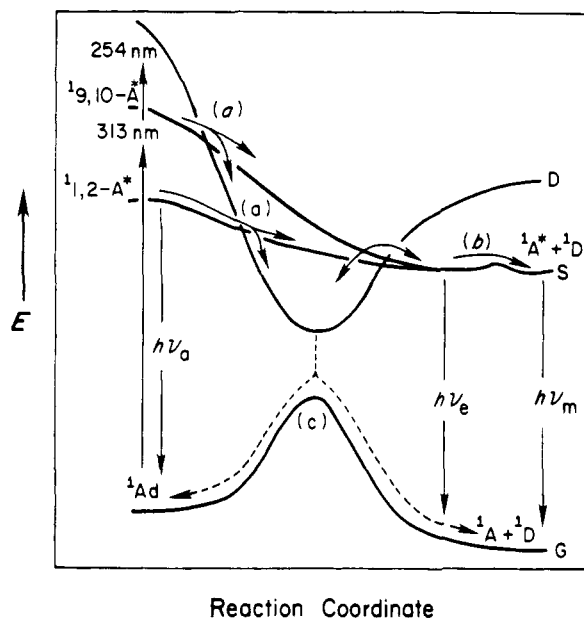


**Figure 1.** Potential energy diagram for [2 + 2] and [4 + 4] cycloreversion illustrating adiabatic ( $a \rightarrow b$ , solid arrows) and diabatic ( $a \rightarrow c$ , broken arrows) photoreaction channels;  $h\nu_a$ ,  $h\nu_e$ , and  $h\nu_m$  designate adduct, exciplex, and addend fluorescence, respectively.

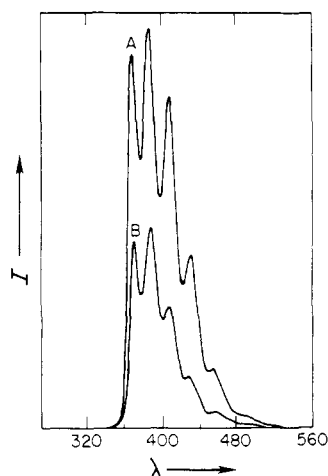


**Figure 2.** Fluorescence spectra (uncorrected) of argon-purged (curve A) and oxygen-saturated (curve B)  $\text{CH}_3\text{CN}$  solutions of 1,2-A,  $7.9 \times 10^{-5}$  M; 320-nm excitation.

absorption profiles (Figure 3). The relative intensity of the DCA-like fluorescence region increases rapidly upon irradiation of 1,2-adduct solutions at  $\lambda < 370$  nm. The extent of 1,2-A photodegradation in the fluorometer was minimized by using narrow excitation slits, high adduct concentrations, short irradiation times, and fresh solutions following each measurement. 1,2-A samples employed for photochemical and spectroscopic measurements had a zero-time DCA content of  $0.15 \pm 0.05\%$  of [1,2-A] (UV, 402 nm). Fluorescence spectra of benzene and pyridine solutions of 1,2-A are red-shifted  $\sim 2$  nm from those in Figure 2.

The fluorescence of acetonitrile and cyclohexane solutions of 9,10-A was examined as a function of excitation wavelength, 240–340 nm, and emission wavelength, 280–560 nm. Only a weak emission identical with DCA fluorescence was detected (Figure 4). Exposure of 9,10-A solutions to the fluorometer excitation beam for prolonged periods of time, e.g., 5–10 min at 270 nm, caused a gradual increase of the intensity of the DCA emission. Due to the presence of trace DCA impurity in 9,10-A samples, excitation of fresh solutions in the 300–390 nm region, where DCA only absorbs, yields DCA fluorescence but at lower intensities than from preirradiated solutions. Comparison of DCA fluorescence intensity from a fresh  $2.4 \times 10^{-4}$  M 9,10-A solution with that from

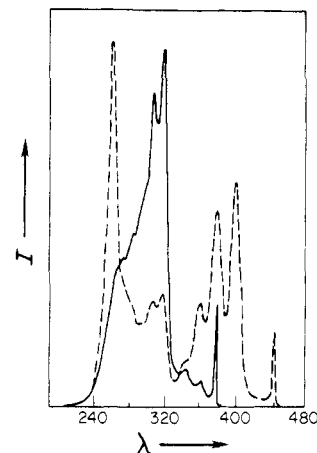


**Figure 3.** Excitation spectra (uncorrected) of air-saturated solutions of 1,2-A,  $3.2 \times 10^{-6}$  M, in  $\text{CH}_3\text{CN}$ : solid curve, monitoring at 383 nm; dashed curve, monitoring at 454 nm.

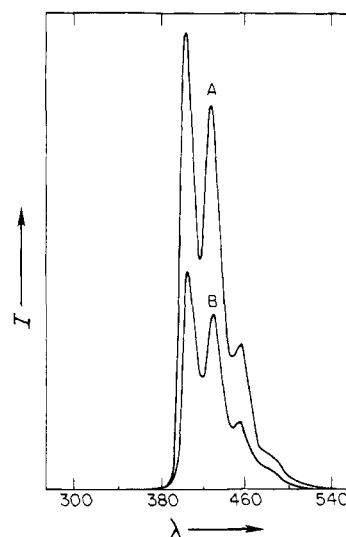


**Figure 4.** Fluorescence spectra (uncorrected) of DCA (curve A) and 9,10-A (curve B) in air-saturated cyclohexane; 270-nm excitation.

**Table I.** Fluorescence Quantum Yields

solvent	DCA, <sup>a</sup> $\phi_f$	1,2-A <sup>b</sup>			9,10-A, <sup>c</sup> $\phi_f$
		$\phi_{ft}$	$\phi_{fa}$	$\phi_{fDCA}$	
$\text{C}_6\text{H}_6$	0.67 <sup>d</sup>	0.037	0.024	0.013	
$\text{C}_6\text{H}_{12}$	0.47				0.0032
$\text{CH}_3\text{CN}$	0.49	0.029	0.017	0.012	0.0020
$\text{C}_5\text{H}_5\text{N}$	0.70	0.034	0.022	0.012	

<sup>a</sup> [DCA]  $\approx 6 \times 10^{-6}$  M; excitation wavelength 340 nm; degassed solutions. <sup>b</sup> [1,2-A]  $\approx 3 \times 10^{-5}$  M; [DCA]  $\approx 5 \times 10^{-4}$  M; excitation wavelength 320 nm; argon-purged solutions. <sup>c</sup> [9,10-A]  $\approx 2 \times 10^{-4}$  M; [DCA]  $\approx 4 \times 10^{-5}$  M; excitation wavelength 270 nm; argon-purged solutions. <sup>d</sup> Used as the standard; average value from ref 9–11.

a standard  $2.4 \times 10^{-6}$  M DCA solution in cyclohexane established that the zero-time DCA content of 9,10-A samples used in all measurements was 0.0009% of [9,10-A]. Excitation spectra of fresh 9,10-A solutions are analogous to the adduct's UV absorption spectrum (Figure 5).

Fluorescence quantum yields were determined at 25.0 °C by using DCA fluorescence in degassed benzene as standard,  $\phi_f = 0.67 \pm 0.03$ <sup>9–11</sup> (Table I). The fluorescence spectra were corrected for nonlinearity of instrumental response and changes in refractive

(9) Bowen, E. J. *Trans. Faraday Soc.* **1954**, *50*, 97.

(10) Dawson, W. R.; Windsor, M. W. *J. Phys. Chem.* **1968**, *72*, 3251.

(11) Saltiel, J.; Townsend, D. E.; Watson, B. D.; Shannon, P. *J. Am. Chem. Soc.* **1975**, *97*, 5688.

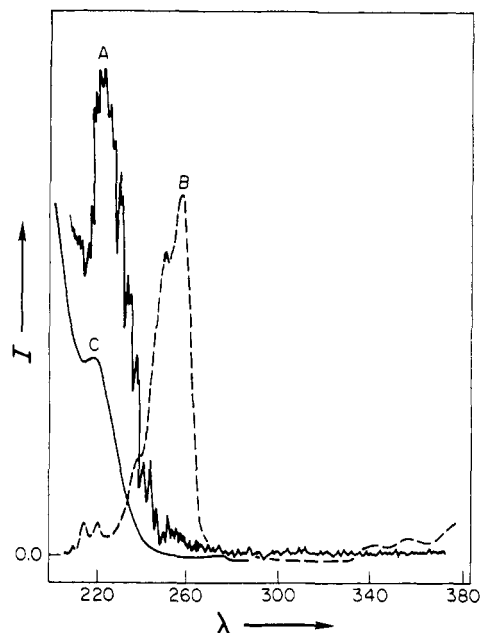


**Figure 5.** Excitation spectra (uncorrected, but Varian SF-330 fluorometer employed) for air-saturated  $C_6H_{12}$  solutions of 9,10-A (curve A) and DCA (curve B), each  $2.4 \times 10^{-6}$  M, monitoring emission at 410 nm. Curve C is 9,10-A's UV absorption profile.<sup>3</sup>

**Table II.** Fluorescence Quenching by Oxygen

solute	conditions <sup>a</sup>	$I_o/I_a^b$	$I_o/I_{ox}^b$
DCA	$CH_3CN$ , 53, 428	$1.38 \pm 0.01$ (1.39)	$2.83 \pm 0.07$
DCA	$C_6H_6$ , 53, 433	$1.34 \pm 0.02$ (1.30)	$2.76 \pm 0.01$
DCA	$C_6H_{12}$ , 2.4, 428 <sup>c</sup>	$1.15 \pm 0.01$	
DCA	$C_6H_5N$ , 53, 434	$1.22 \pm 0.01$ (1.17)	$2.00 \pm 0.02$
1,2-A	$CH_3CN$ , 79, 382	$1.21 \pm 0.01$	$2.04 \pm 0.04$
1,2-A	$C_6H_6$ , 76, 383	$1.26 \pm 0.01$	$2.34 \pm 0.04$
1,2-A	$C_6H_5N$ , 79, 385	$1.11 \pm 0.01$	$1.54 \pm 0.01$
9,10-A	$CH_3CN$ , 244, 428 <sup>c</sup>	$1.31 \pm 0.06$	$2.85 \pm 0.01$
9,10-A	$C_6H_{12}$ , 238, 428 <sup>c</sup>	$1.15 \pm 0.03$	

<sup>a</sup> Solvent and solute concentration in  $\mu M$ ; monitoring wavelength in nm; 25.0 °C throughout; excitation wavelength 320 nm unless noted otherwise. <sup>b</sup> Error limits are average deviations from the mean of two or more determinations; numbers in parentheses obtained relative to degassed solution  $I_o$ 's. <sup>c</sup> Excitation at 270 nm, filter system 1; see Experimental Section.

index.<sup>12</sup> Identical emission intensities were obtained from degassed or argon-purged DCA solutions. Corrected fluorescence spectra from 1,2-A were decomposed into <sup>1</sup>1,2-A\* and <sup>1</sup>DCA\* emission contributions by attributing all emission at  $\lambda \geq 485$  nm to DCA fluorescence, e.g., Figure 6. This allowed separation of total fluorescence quantum yields,  $\phi_{ft}$ , into 1,2-A,  $\phi_{fa}$ , and DCA,  $\phi_{fDCA}$ , components (Table I).

Relative emission intensities of argon-,  $I_o$ , air-,  $I_a$ , and oxygen-purged,  $I_{ox}$ , solutions are shown in Table II. In the case of 1,2-A the effect of oxygen depends on the emission wavelength (Table III).

The effect of DCA contamination on the fluorescence yield of 9,10-A was determined by measuring relative emission intensities of air-saturated cyclohexane solutions of 9,10-A with and without added DCA (Table IV). The emission intensity of these solutions for 340-nm excitation where only DCA absorbs was shown to be proportional to [DCA].<sup>13</sup> For  $[9,10-A] = 2.38 \times 10^{-4}$  M, the undoped solution was found to contain  $2.06 \times 10^{-9}$  M DCA, which increased to  $4.94 \times 10^{-9}$  M under the conditions used in obtaining a single fluorescence spectrum (270 nm, filter 1, ~2 min).

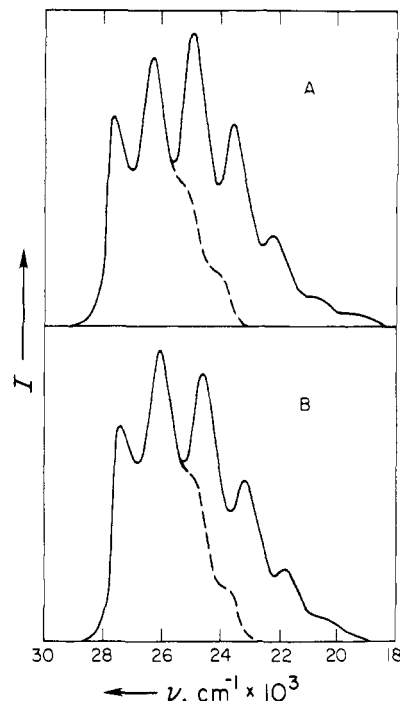


**Figure 6.** Corrected fluorescence spectra of argon-purged  $CH_3CN$  (curve A) and  $C_6H_6$  (curve B) solutions; 320-nm excitation. Dashed curves obtained by subtraction of DCA fluorescence from the total spectrum.

**Photochemical Observations. (A) Product Studies.** Benzene- $d_6$  and cyclohexane- $d_{12}$  solutions of the adducts were degassed in NMR tubes, flame-sealed at a constriction, and the progress of the photoreactions (~23 °C) was followed by <sup>1</sup>H NMR, 270 MHz. Tetramethylsilane, ~0.003 M, and cyclohexane- $d_{11}$  <sup>1</sup>H resonances were employed as internal standards (Table V). At conversions below 20%, loss of 1,2-A equals DCA and CHD yields within the experimental uncertainty of the measurements ( $\pm 10\%$ ) for either 254- or 313-nm excitation. At higher conversions DCA and CHD yields do not account for adduct loss, probably due to secondary photochemical reactions. The <sup>1</sup>H NMR spectrum of 1,2-A which was irradiated at 254 nm to 55% conversion in  $C_6D_{12}$  showed (in addition to strong DCA and CHD signals) weak multiplets centered at  $\delta$  3.2–5.2,  $\delta$  4.8–5.2, and  $\delta$  7.2 which do not correspond to any of the other known photoadducts. GLC analysis of this solution gave peaks with retention times identical with those of 9-chloroanthracene, MCA (2.2% relative area), DCA (43%), 9,10-A (1.5%), and 1,2-A (49%) as well as two peaks (~2.5% each) with retention times similar to 9,10-A. The multiplets of the unknown photoproduct(s) were not discernible in NMR spectra of 1,2-A solutions irradiated (254 nm) to ~25% conversion. NMR spectra of  $C_6D_{12}$  solutions of 9,10-A irradiated (254 nm) to 24–59% conversion show weak resonances corresponding to DCA and CHD (8% of 9,10-A consumed), a multiplet at  $\delta$  3.0, and strong broad signals comprised of several overlapping multiplets at  $\delta$  5.4–5.6 and  $\delta$  6.6–7.5. Once again, these unassigned resonances do not correspond to any of the other known photoadducts. GLC analysis of a 9,10-A  $C_6D_{12}$  solution irradiated (254 nm, filter 3) to ~56% conversion (NMR) showed peaks with retention times identical with those of MCA (3.7%, relative area), DCA (0.9%), 9,10-A (76%), and 1,2-A (~0.3%), as well as a GLC peak (17%) with a retention time between those of DCA and 9,10-A and three small peaks (~0.7% each) with retention times similar to that of 1,2-A.

**(B) Quantum Yields.** 1,2-A loss and DCA quantum yields for 254-nm excitation in  $CH_3CN$  and 313-nm excitation in  $CH_3CN$ ,  $C_6H_6$ , and  $C_6H_5N$  were determined for degassed and air-saturated solutions (Table VI). Irradiations were conducted in a Moses merry-go-round apparatus<sup>14</sup> at  $25.0 \pm 0.1$  °C. The direct pho-

(12) (a) Parker, C. A. "Photoluminescence of Solutions"; Elsevier: Amsterdam, 1968. (b) Correction factors determined by Marinari A. (see: Marinari, A.; Saltiel, J. *Mol. Photochem.* **1976**, *7*, 225).

(13) Calvert, J. G.; Pitts, J. N. "Photochemistry"; Wiley: New York, 1966; pp 800–801.

(14) Moses, F. G.; Liu, R. S. H.; Monroe, B. M. *Mol. Photochem.* **1969**, *1*, 245.

Table III. Wavelength Dependence of Oxygen Quenching of 1,2-A Emission<sup>a</sup>

emission band <sup>b</sup>	CH <sub>3</sub> CN			C <sub>6</sub> H <sub>6</sub>			C <sub>5</sub> H <sub>5</sub> N		
	λ <sub>max</sub> <sup>c</sup>	I <sub>0</sub> /I <sub>a</sub>	I <sub>0</sub> /I <sub>ox</sub>	λ <sub>max</sub> <sup>c</sup>	I <sub>0</sub> /I <sub>a</sub>	I <sub>0</sub> /I <sub>ox</sub>	λ <sub>max</sub> <sup>c</sup>	I <sub>0</sub> /I <sub>a</sub>	I <sub>0</sub> /I <sub>ox</sub>
0-0	365	1.23	1.99	365	1.28	2.33	366	1.11	1.53
0-1	382	1.23	1.99	383	1.26	2.31	385	1.11	1.54
0-0'	404	1.38	2.65	405	1.39	2.81	406	1.18	1.79
0-1'	428	1.50	3.36	429	1.48	3.42	432	1.24	2.07
0-2'	454	1.55	3.59	456	1.52	3.68	456	1.27	2.16

<sup>a</sup> Samples and conditions described in Table II. <sup>b</sup> Primed bands assigned to <sup>1</sup>DCA\*. <sup>c</sup> Emission wavelength in nm.Table IV. Relative Fluorescence Intensities of 9,10-A Solutions Doped with DCA<sup>a</sup>

[DCA], M	[DCA]/[DCA] <sub>0</sub>	I <sub>d</sub> /I <sub>0</sub> <sup>b</sup>
2.06 × 10 <sup>-9</sup>	1.00	1.00
5.43 × 10 <sup>-8</sup>	26.4	1.18
6.32 × 10 <sup>-7</sup>	307	3.10
1.55 × 10 <sup>-6</sup>	752	6.15

<sup>a</sup> Air-saturated C<sub>6</sub>H<sub>12</sub>; 25.0 °C; [9,10-A] = 2.38 × 10<sup>-4</sup> M; excitation at 270 nm (filter 1); emission at 405 nm. <sup>b</sup> Ratio of doped to undoped fluorescence intensity.Table V. Photoproduct Distribution, 270-MHz <sup>1</sup>H NMR<sup>a</sup>

solvent	adduct; M	adduct loss, % <sup>b</sup>	% product appearance	
			DCA	CHD
C <sub>6</sub> D <sub>6</sub>	1,2-A; 0.033 <sup>c</sup>	6.5 ± 1	6.2 ± 1	6.2 ± 1
C <sub>6</sub> D <sub>6</sub>	1,2-A; 0.033 <sup>c</sup>	12.7 ± 1	13.2 ± 2	10.9 ± 2
C <sub>6</sub> D <sub>6</sub>	1,2-A; 0.033 <sup>c</sup>	47.0 ± 6	31.2 ± 4	28.0 ± 4
C <sub>6</sub> D <sub>12</sub>	1,2-A; 0.034 <sup>d</sup>	22.6 ± 3	19.7 ± 2	19.7 ± 2
C <sub>6</sub> D <sub>12</sub>	1,2-A; 0.034 <sup>d</sup>	29.1 ± 3	22.6 ± 2	22.6 ± 2
C <sub>6</sub> D <sub>12</sub>	1,2-A; 0.034 <sup>d</sup>	54.9 ± 5	37.1 ± 4	37.1 ± 4
C <sub>6</sub> D <sub>12</sub>	9,10-A; 0.034 <sup>e</sup>	59.0 ± 6	4.4 ± 1	4.4 ± 1

<sup>a</sup> Degassed NMR tubes; ~23 °C. <sup>b</sup> Relative to initial adduct concentration; error limits reflect precision in NMR integration. <sup>c</sup> 313 nm, filter 2. <sup>d</sup> 254 nm, filter 3. <sup>e</sup> 254 nm, filter 4.

toisomerization of *trans*-stilbene in degassed acetonitrile was used for actinometry;  $\phi_{\text{isc}} = 0.51 \pm 0.02$  reported<sup>15,16</sup> for *n*-pentane, 313 nm, was assumed to apply for acetonitrile. Stationary states for stilbene photoisomerization in CH<sub>3</sub>CN were shown to be 45.7 ± 0.1% *cis*, 254 nm, 8.92 × 10<sup>-4</sup> M stilbene, and 91.2 ± 0.1% *cis*, 313 nm, 4.46 × 10<sup>-4</sup> M stilbene. These values are very close to those reported for *n*-pentane and were used for back-reaction corrections.<sup>15</sup> Corrected conversions to *cis*-stilbene ranged from 4.49 to 9.72%. When necessary, larger conversions were avoided by irradiating two actinometer solutions in series with the same adduct sample, and the initial [*trans*-stilbene] was adjusted from 4.46 × 10<sup>-4</sup> to 8.92 × 10<sup>-4</sup> M.<sup>17</sup> Results from duplicate actinometer samples irradiated in parallel were in excellent agreement. Freshly irradiated solutions were analyzed for 1,2-A loss and DCA appearance by UV spectroscopy, monitoring 1,2-A at λ<sub>max</sub> ≈ 320 nm and DCA at λ<sub>max</sub> ≈ 402 nm;<sup>3</sup> conversions ranged between 5.88 and 13.1%.

Solutions of 9,10-A in degassed and air-saturated cyclohexane were irradiated (254 nm) in parallel with 1,2-A solutions. DCA formation was monitored by UV absorption in this case also. UV spectra of irradiated 9,10-A solutions show, in addition to DCA absorption, two weak bands centered at 306 and 318 nm similar to those of 1,2-A. Assuming that the unknown product has the same absorptivity coefficient as 1,2-A gives  $\phi \approx 1/3 \phi_{\text{DCA}}$ . In the presence of air the 306–318 nm region could not be analyzed due to an additional broad shoulder at λ < 340 nm. Conversions to DCA ranged from 0.0343 to 0.0675%, and by inference from the NMR observations (see above), 9,10-A loss was less than 1%.

Table VI. Adduct Loss and DCA Formation Quantum Yields

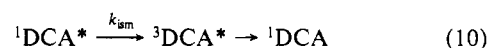
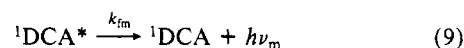
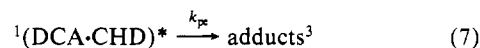
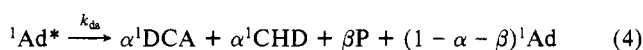
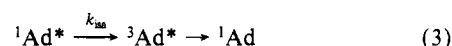
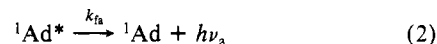
adduct <sup>a</sup>	λ <sub>exc</sub> , nm <sup>b</sup>	solvent	φ <sub>-A</sub> <sup>c</sup>	φ <sub>DCA</sub> <sup>c</sup>
1,2-A	254	CH <sub>3</sub> CN	0.32	0.30
1,2-A	254	CH <sub>3</sub> CN <sup>d</sup>	0.25 ± 0.01	0.25 ± 0.02
1,2-A	313	CH <sub>3</sub> CN	0.36 ± 0.02	0.35 ± 0.04
1,2-A	313	CH <sub>3</sub> CN <sup>d</sup>	0.28 ± 0.01	0.26 ± 0.01
1,2-A	313	C <sub>6</sub> H <sub>6</sub>	0.27 ± 0.05	0.27 ± 0.03
1,2-A	313	C <sub>6</sub> H <sub>6</sub> <sup>d</sup>	0.21 ± 0.01	0.18 ± 0.01
1,2-A	313	C <sub>5</sub> H <sub>5</sub> N	0.31 ± 0.01	0.30 ± 0.03
1,2-A	313	C <sub>5</sub> H <sub>5</sub> N <sup>d</sup>	0.28 ± 0.01	0.24 ± 0.01
9,10-A	254	C <sub>6</sub> H <sub>12</sub> <sup>d</sup>	1.0 <sup>e</sup>	0.11 ± 0.01
9,10-A	254	C <sub>6</sub> H <sub>12</sub> <sup>d</sup>		0.11

<sup>a</sup> [1,2-A]<sub>0</sub> = 4.55 × 10<sup>-4</sup> or 4.6 × 10<sup>-4</sup> M; [9,10-A]<sub>0</sub> = 0.0385 M.<sup>b</sup> Excitation at 254 nm, filter 5; excitation at 313 nm, filter 6.<sup>c</sup> Uncertainties are average deviations from the mean of two or more independent determinations. <sup>d</sup> Air-saturated solutions.<sup>e</sup> From φ<sub>-A</sub>/φ<sub>DCA</sub> from NMR experiments.

Quantum yields are reported in Table VI.

## Discussion

The results described above will be discussed in terms of the mechanism



where Ad is an adduct, P represents unknown products, <sup>1</sup>(DCA·CHD)\* is the singlet exciplex, and all other symbols are self-explanatory. Equations 6–10 have been discussed in accounting for the DCA/CHD cycloaddition reactions.<sup>3</sup> Reference to Figure 1 shows that pericyclic minima on the D surface are proposed intermediates for adiabatic cleavage. Our results do not require involvement of these intermediates, so they are not explicitly included in the mechanism.

**Spectroscopic Observations.** The emission and excitation spectra of 9,10-A reveal unequivocally the existence of an adiabatic reaction channel in its photocleavage (Figures 4 and 5). Furthermore, the DCA doping experiments (Table IV) show that all fluorescence observed following its excitation is due to <sup>1</sup>DCA\* formed via this channel and not by excitation of the miniscule amount of DCA present as a contaminant.

(15) Saltiel, J.; Marinari, A.; Chang, D. W.-L.; Mitchener, J. C.; Megarity, E. D. *J. Am. Chem. Soc.* **1979**, *101*, 2982.

(16) Malkin, S.; Fischer, E. *J. Phys. Chem.* **1964**, *68*, 1153.

(17) A detailed description of the results is given in Smothers, W. K., Ph.D. Dissertation, The Florida State University, Tallahassee, Florida, 1981.

DCA contamination of 1,2-A is more serious and significantly contributes to the fluorescence measurements especially when excitation is in regions where DCA absorbs strongly (Figures 2 and 3). The excitation spectrum obtained by monitoring emission at 383 nm is analogous to the UV absorption profile of 1,2-A as expected for emission originating entirely from  $^1\text{1,2-A}^*$ . On the other hand, monitoring DCA emission at 454 nm gives an excitation spectrum which resembles a mixture of DCA and 1,2-A absorption spectra. Since  $^1\text{1,2-A}^*$  does not emit at 454 nm (Figure 6), the appearance of the adduct-like absorption profile in the 300–330 nm region of the excitation spectrum suggests strongly an adiabatic pathway to  $^1\text{DCA}^*$  from  $^1\text{1,2-A}^*$ . This conclusion is confirmed by the influence of molecular oxygen on the total fluorescence envelope of 1,2-A solutions. Inspection of Figure 2 and Table III shows that  $^1\text{DCA}^*$  fluorescence quenching is more pronounced than  $^1\text{1,2-A}^*$  fluorescence quenching. Furthermore, since  $^1\text{DCA}^*$  fluorescence generated by excitation of 1,2-A solutions is quenched more strongly than fluorescence generated by exciting DCA directly (compare Tables II and III), at least part of the DCA fluorescence from the 1,2-A solutions must derive from adiabatic cleavage of  $^1\text{1,2-A}^*$ . This conclusion can be understood by including the following quenching steps in the mechanism:



Application of the steady-state approximation to all excited species in eq 1–13 gives

$$\left(\frac{I_0}{I}\right)_\lambda = \left[ \frac{\sigma_\lambda}{1 + k_{qa}\tau_a[\text{O}_2]} + \frac{1 - \sigma_\lambda}{(1 + k_{qa}\tau_a[\text{O}_2])(1 + k_{qe}\tau_e[\text{O}_2])(1 + k_{qm}\tau_m[\text{O}_2])} \right]^{-1} \quad (14)$$

where  $\tau_a = (k_{fa} + k_{isa} + k_{da} + k_{ea})^{-1}$ ,  $\tau_e = (k_{-e} + k_{de} + k_{pe})^{-1}$  and  $\tau_m = (k_{fm} + k_{ism})^{-1}$  are the lifetimes of  $^1\text{Ad}^*$ ,  $^1(\text{DCA}\cdot\text{CHD})^*$  at  $[\text{CHD}] = 0$ , and  $^1\text{DCA}^*$ , respectively, and  $\sigma_\lambda$  is the fraction of light emitted by  $^1\text{Ad}^*$  at a specific wavelength  $\lambda$  in the absence of  $\text{O}_2$ . This expression can be simplified since the exciplex, to the extent that it participates in the cycloaddition reaction, is non-emitting and too short-lived to be quenched by oxygen, i.e.,  $k_{qe}\tau_e[\text{O}_2] \approx 0$ .<sup>3</sup> Inspection of Figure 6 shows that  $\sigma_\lambda = 1$  for 0,0 and 0,1 bands of  $^1\text{Ad}^*$  fluorescence. It follows that at those wavelengths eq 14 reduces to

$$\left(\frac{I_0}{I}\right)_{0,0} = \left(\frac{I_0}{I}\right)_{0,1} = 1 + k_{qa}\tau_a[\text{O}_2] \quad (15)$$

the ordinary Stern–Volmer relationship, as is borne out by the results in Table III. Similarly, it can be seen that emission at the 0,2' band corresponds to the limiting condition of  $\sigma_\lambda = 0$  which when applied to eq 14 along with  $k_{qe}\tau_e[\text{O}_2] = 0$ , gives

$$\left(\frac{I_0}{I}\right)_{0,2'} = (1 + k_{qa}\tau_a[\text{O}_2])(1 + k_{qm}\tau_m[\text{O}_2]) \quad (16)$$

Should other intermediates, such as pericyclic minima of the D state(s), lie in the path to  $^1\text{DCA}^*$  and should these also be quenched by oxygen, the oxygen effect would be larger than predicted by eq 16. Since the first term in eq 16 is known from eq 15 and the second term describes the effect of oxygen on directly excited DCA, eq 16 can be expressed as  $(I_0/I)_{0,2'} = (I_0/I)_{0,0'} (I_0/I)_{\text{DCA}}$  which are quantities given in Tables II and III. Values calculated in this way (Table VII) are generally larger than the observed values which are nevertheless significantly larger than experimental values for directly excited  $^1\text{DCA}^*$ . While these observations establish an adiabatic pathway to  $^1\text{DCA}^*$ , they require that part of the  $^1\text{DCA}^*$  emission from 1,2-A solution excited

Table VII. Calculated Oxygen Effects on Fluorescence of  $^1\text{DCA}^*$  Formed Adiabatically from  $^1\text{1,2-A}^*$ <sup>a</sup>

solvent	$I_0/I_a$	$\xi_a^b$	$I_0/I_{ox}$	$\xi_{ox}^b$
$\text{CH}_3\text{CN}$	$1.68 \pm 0.02$	0.63	$5.77 \pm 0.18$	0.42
$\text{C}_6\text{H}_6$	$1.66 \pm 0.03$	0.57	$6.46 \pm 0.11$	0.44
$\text{C}_5\text{H}_5\text{N}$	$1.33 \pm 0.04$	0.41	$3.08 \pm 0.04$	0.21

<sup>a</sup> Using eq 16 and the observations in Tables II and III; ranges are standard deviations. <sup>b</sup> See ref 18.

at 320 nm arise by direct excitation of DCA present as an impurity. More specifically, simple algebraic manipulation of the expected and observed  $I_0/I$  values in Tables II, III, and VII for air-saturated solutions gives 0.63, 0.57, and 0.41 as the fractions of  $^1\text{DCA}^*$  emission observed from 1,2-A solutions in  $\text{CH}_3\text{CN}$ ,  $\text{C}_6\text{H}_6$ , and  $\text{C}_5\text{H}_5\text{N}$ , respectively, which originates from 1,2-A excitation.<sup>18</sup> Somewhat lower DCA fluorescence contributions from 1,2-A excitation are predicted from the observations in oxygen-saturated solutions. It follows that approximately half of the  $\phi_{\text{DCA}}$  values given for 1,2-A in Table I are due to adiabatic cleavage of  $^1\text{1,2-A}^*$ . Sequential oxygen quenching effects have also been observed in the intramolecular adiabatic photocycloreversion of dimethyllepidoptere.<sup>7b</sup>

In contrast to the results with 1,2-A, relative  $^1\text{DCA}^*$  emission intensities of argon-purged air- and oxygen-saturated 9,10-A solutions are, within the precision of the measurements, identical with those obtained by direct excitation of  $^1\text{DCA}$  (Table II). It follows that the lifetime of the obligatory precursor  $^9\text{10-A}^*$ , as well as the lifetimes of any other excited-state intermediates in the  $^9\text{10-A}^* \rightarrow ^1\text{DCA}^*$  path, is too short ( $\tau < 1$  ns) to be quenched by oxygen; i.e.,  $k_{qa}\tau_a[\text{O}_2] \ll 1$  in eq 16. This conclusion is consistent with measurements made on the 9,10-adduct obtained from 9-cyanoanthracene, CNA, and CHD. In this system  $^1\text{CNA}^*$  is observed in absorption within 33 ps of adduct excitation.<sup>7c</sup> It is also consistent with our inability to detect fluorescence directly from  $^9\text{10-A}^*$ ,  $\phi_{fa} < 10^{-4}$ . The oxygen effect on 9,10-A-derived  $^1\text{DCA}^*$  fluorescence is reminiscent of observations on the photocleavage of 9-methylanthracene,  $^1\text{MA}$ , dimer. In that case too,  $I_0/I_{ox}$  ratios for fluorescence from  $^1\text{MA}^*$  formed adiabatically from the singlet excited dimer,  $^1\text{MA}_2^*$ , or by direct  $^1\text{MA}$  excitation are identical in  $\text{CH}_3\text{CN}$ .<sup>19</sup> However, since a fluorescent excimer also forms adiabatically from  $^1\text{MA}_2^*$  and should also be quenched by oxygen (the magnitude of this effect was, unfortunately, not reported), enhanced oxygen quenching of  $^1\text{MA}^*$  fluorescence would be expected on the basis of the  $^1\text{MA}_2^* \rightarrow ^1(\text{MA}\cdot\text{MA})^* \rightarrow ^1\text{MA}^* + \text{MA}$  sequence.<sup>19</sup> In the absence of such enhancement it was concluded that singlet excimer and  $^1\text{MA}^*$  form from  $^1\text{MA}_2^*$  by independent adiabatic channels.<sup>19</sup> Further elaboration on this mechanism has been based on the temperature dependencies of fluorescence quantum yields and lifetimes of  $^1\text{MA}_2^*$ ,  $^1(\text{MA}\cdot\text{MA})^*$ , and  $^1\text{MA}^*$  in hydrocarbon solvents.<sup>20</sup> Since the DCA·CHD exciplex is nonfluorescent and short-lived,<sup>3</sup> our observations do not explicitly address the interesting possibility of an independent adiabatic channel from either adduct  $\text{S}_1$  state to  $^1\text{DCA}^*$ ; since it is not needed in accounting for the results, it has been excluded from the mechanism.

According to the mechanism in eq 1–10, the quantum yields of adiabatically formed  $^1\text{DCA}^*$  are given by

$$\phi_{^1\text{DCA}^*} = \phi_{\text{DCA}} / \phi_{\text{fm}} = k_{ea}\tau_a k_{-e}\tau_e \quad (17)$$

where  $\phi_{\text{fm}}$  is the quantum yield of DCA fluorescence from directly excited DCA.<sup>21</sup> Values of  $\phi_{^1\text{DCA}^*}$ , calculated from the data in Tables I and VII, are shown in Table VIII. Stern–Volmer plots for the quenching of  $^1\text{DCA}^*$  fluorescence by CHD have yielded

(18) The expression used in these calculations is  $(I/I_0)_{\text{obsd}} = \xi/(I_0/I)_{\text{adiab}} + (1 - \xi)/(I_0/I)_{\text{direct}}$ , where  $\xi$  is the fraction of DCA fluorescence originating by 1,2-A excitation.

(19) Menter, J.; Förster, Th. *Photochem. Photobiol.* **1972**, *15*, 289.

(20) Yamamoto, S.; Grellmann, K.-H.; Weller, A. *Chem. Phys. Lett.* **1980**, *70*, 241.

(21)  $^1\text{DCA}^*$  quenching by product CHD is negligible due to the low adduct concentrations and low conversions employed.<sup>3</sup>

**Table VIII.** Quantum Yields and Related Parameters for Adiabatic  $^1\text{DCA}^*$  Formation from the Adducts

solvent	adduct	$\phi_{^1\text{DCA}^*}^a$	$\tau_a, \text{ns}^b$	$k_{-e}\tau_e^c$	$k_{ea}\tau_a^d$
$\text{CH}_3\text{CN}$	1,2-A	0.015	$5.8 \pm 0.15$	0.92	0.017
$\text{C}_6\text{H}_6$	1,2-A	0.011	$7.7_0 \pm 0.26$	0.98	0.011
$\text{C}_5\text{H}_5\text{N}$	1,2-A	0.0070	$5.0_6 \pm 0.06$	0.76	0.009 <sub>2</sub>
$\text{CH}_3\text{CN}$	9,10-A	0.0041		0.92	0.004 <sub>3</sub>
$\text{C}_6\text{H}_{12}$	9,10-A	0.0068		0.98 <sup>e</sup>	0.006 <sub>9</sub>

<sup>a</sup> Values of  $\phi_{^1\text{DCA}^*}$  for 1,2-A corrected by using  $\xi_a$  from Table VII. <sup>b</sup> Based on  $\text{O}_2$  quenching of  $^1\text{1,2-A}^*$  fluorescence; see the text. <sup>c</sup> From ref 3. <sup>d</sup> Using eq 17. <sup>e</sup> Assumed identical with the  $\text{C}_6\text{H}_6$  value.

$pk_e\tau_m$  values, where  $p$  is the fraction of exciplexes which do not regenerate  $^1\text{DCA}^*$ .<sup>3</sup> Lower limits for  $p$ , estimated from the deviation of  $pk_e$  from values of diffusion-controlled rate constants,<sup>3</sup> were used to calculate  $k_{-e}\tau_e = 1 - p$  and, by using eq 17,  $k_{ea}\tau_a$  values shown in Table VIII. Also shown in Table VIII are  $\tau_a$  values for 1,2-A obtained from  $I_0/I_a$  and  $I_0/I_{ox}$  data by assuming  $k_{qa} = k_{qm}$  in eq 11 and 12. It follows that  $k_{ea} = 2.90 \times 10^6$ ,  $1.4 \times 10^6$ , and  $1.8 \times 10^6 \text{ s}^{-1}$  in  $\text{CH}_3\text{CN}$ ,  $\text{C}_6\text{H}_6$ , and  $\text{C}_5\text{H}_5\text{N}$ , respectively. Of mechanistic significance is the observation that the effect of changing the solvent from benzene to pyridine on  $\phi_{^1\text{DCA}^*}$  appears to be dictated primarily by the change in  $k_{-e}\tau_e$ , consistent with sequential formation of  $^1(\text{DCA}\cdot\text{CHD})^*$  and  $^1\text{DCA}^*$  from  $^1\text{1,2-A}^*$ . Increasing the polarity of the solvent to acetonitrile causes a modest increase in  $k_{ea}$ . A similar, but much more pronounced, effect may be operating in the case of the  $^1\text{MA}$  dimer, for which  $^1\text{MA}^*_2$  fluorescence is observed in hydrocarbon solvents<sup>20</sup> but is absent in acetonitrile.<sup>19</sup>

**Photochemical Observations.** Irradiation of a 1:1 mixture of 1,2-A and 1,4-A in cyclohexane at 366 nm has been reported to selectively destroy 1,2-A (yield DCA:  $72 \pm 2\%$ ).<sup>3</sup> Product distributions (Table V) and quantum yields (Table VI) obtained in this work show that DCA and CHD are obtained in 1:1 relative yield from 1,2-A (313 nm) or 9,10-A (254 nm) but with markedly different efficiencies. At low conversions, cleavage of 1,2-A to DCA and CHD proceeds quantitatively for 313-nm excitation and nearly quantitatively ( $\sim 90\%$ ) for excitation at 254 nm. In the case of 9,10-A, a complex mixture of products is obtained and cleavage to DCA and CHD accounts for only 8–11% of the consumed adduct. Photochemical conversion of 1,2-A or 9,10-A to the other photoadducts could not be detected by NMR analysis even at high conversions, but UV absorption spectra reveal the possible formation of 1,2-A as a minor photoproduct,  $\phi_{1,2-A} \leq 0.037$ , from 9,10-A.

Comparison of  $\phi_{^1\text{DCA}^*}$  and  $\phi_{\text{DCA}}$  values (Tables II and VIII) shows that for both adducts adiabatic cleavage to  $^1\text{DCA}^*$  accounts for only 2–6% of the total  $^1\text{DCA}$  formed; clearly, diabatic reaction channels to  $^1\text{DCA}$  predominate. If the exciplex is an essential intermediate in the paths to  $^1\text{DCA}^*$  as shown in the mechanism and Figure 1, and to the photoadducts generally,<sup>3</sup> then some adduct photoisomerization via the exciplex would be expected

$$\phi_{\text{Ad}_i} = p \phi_{\text{Ad}_i}^{\text{lim}} k_{ea}\tau_a \quad (18)$$

where  $\phi_{\text{Ad}_i}^{\text{lim}}$  is the limiting appearance quantum yield of adduct  $i$  at infinite diene concentration in the DCA/CHD system. Experimentally determined  $p$ ,<sup>3</sup>  $\phi_{\text{Ad}_i}^{\text{lim}}$ , and  $k_{ea}\tau_a$  values (Table VIII) give  $\phi_{\text{Ad}_i}$  values 3–5 orders of magnitude smaller than observed adduct loss quantum yields. It follows that adiabatic formation of the singlet exciplex should result in yields of its characteristic products too low to allow their detection by NMR analysis, consistent with our observations. On the other hand, if the UV absorption bands at 306 and 318 nm, observed upon irradiation of 9,10-A in degassed cyclohexane, correspond to 1,2-A, the resulting  $\phi_{1,2-A}$  value of  $0.037 \pm 0.002$  is substantially larger than predicted by eq 18,  $\phi_{1,2-A} \approx 2 \times 10^{-5}$ . Though 1,2-A would still

be a minor photoproduct from 9,10-A, the possible involvement of a diabatic reaction channel from  $^1\text{9,10-A}^*$  to 1,2-A which bypasses the singlet exciplex is intriguing. In any case, it seems safe to conclude that interconversion between pericyclic minima on the **D** surface does not play a significant role in the deactivation of  $^1\text{1,2-A}^*$  and  $^1\text{9,10-A}^*$ .

The effect of oxygen on  $\phi_{-A}$  and  $\phi_{\text{DCA}}$  is consistent with the mechanism eq 1–13. For 1,2-A,  $\phi_{-A}^0/\phi_{-A}^a$  and  $\phi_{\text{DCA}}^0/\phi_{\text{DCA}}^a$  ratios (Table VI) are in close agreement with  $I_0/I_a$  ratios obtained for  $^1\text{1,2-A}^*$  fluorescence (Tables II and III). Similarly, for 9,10-A, for which  $I_0/I_a = 1.00$  was inferred from the effect of air on the fluorescence of adiabatically generated  $^1\text{DCA}^*$ ,  $\phi_{\text{DCA}}^0/\phi_{\text{DCA}}^a = 1.00$ . Since oxygen quenching should provide an efficient decay channel for adduct triplets, the agreement between  $\phi_{-A}^0/\phi_{-A}^a$ ,  $\phi_{\text{DCA}}^0/\phi_{\text{DCA}}^a$  and  $I_0/I_a$  ratios suggests either that they are not involved in the photochemistry of the adducts or that they are unusually short-lived and not measurably quenched by  $\text{O}_2$  in air-saturated solutions.

## Experimental Section

**Materials.** All materials used in this work have been described previously.<sup>3</sup>

**Fluorescence Measurements.** A Perkin-Elmer Hitachi MPF-2A spectrophotometer was employed in the ratio recording mode as previously described.<sup>3</sup> Slit band-passes were typically set at 4–7 and 5–10 nm for excitation and emission, respectively. Streams of argon, air, or oxygen were gently bubbled through the solutions for 120 s (timed) directly in  $1 \times 1 \times 5 \text{ cm}$  quartz cells, which were then Teflon stoppered. No change in the oxygen content of the solutions was noted while measurements were being made. Degassed solutions and argon-bubbled solutions of DCA gave identical fluorescence intensities. Relative fluorescence quantum yields were determined at  $25.0 \pm 0.1^\circ \text{C}$  by using fresh solutions with carefully matched absorbances (5.0-cm UV cells were employed for absorbance matching). Relative emission intensities, corrected for non-linearity of instrumental response, were plotted vs.  $\text{cm}^{-1}$  and relative areas determined by cutting and weighing Xerox copies of the spectra.<sup>12</sup> A few fluorescence excitation spectra were measured at room temperature ( $\sim 23^\circ \text{C}$ ) by using a Varian SF-330 spectrofluorometer (courtesy Dr. M. Kasha) which has a flatter response than the Hitachi spectrophotometer over the region of interest.

**Irradiation Procedures.** A merry-go-round apparatus<sup>14</sup> was employed for quantum yield measurements as previously described.<sup>3</sup> Quartz ampoules (13-mm o.d.) and NMR tubes (3-mm o.d.) were used for 254-nm irradiations, and Pyrex ampoules and NMR tubes were used for 313-nm irradiations.

**Lamps and Light Filters.** A Nester-Faust low-pressure mercury lamp was used for 254-nm excitation, and Hanovia medium-pressure mercury lamps (200- and 550-W, Ace Glass, Inc.) were used for 313-nm excitation. Filter system 1 consisted of a 1.0 cm pathlength UV cell filled with aqueous potassium iodide, 0.02 g/mL, and a 1.0-cm UV cell filled with 1 atm of chlorine gas. The two cells were arranged in series so that light from the Hitachi fluorometer excitation beam entered the KI solution first. This filter system removes all light at 300–370 nm and  $<265 \text{ nm}$  and was used to minimize inadvertent DCA excitation when exciting 9,10-A solutions with the Hitachi monochromator set at 270 nm. Filter system 2 consisted of a 500-mL aqueous solution of  $\text{K}_2\text{Cr}_2\text{O}_7$  (0.734 g) and  $\text{K}_2\text{CO}_3$  (15.0 g) transmitting a narrow band of light at 313 nm and visible light at  $\lambda > 450 \text{ nm}$  and Corning CS 7-54 glass filter plates which remove visible light at  $\lambda > 430 \text{ nm}$ . The solution was contained in a Pyrex Hanovia reactor-probe assembly, 0.2–0.3 cm pathlength, equipped with a 550-W Hanovia lamp. Filter system 3 consisted of 2 atm of  $\text{Cl}_2$  sealed in the cooling jacket of a quartz Hanovia probe, 1-cm path length, and a cylindrical Vycor sleeve. Filter system 4 was as in filter system 3 except 1 atm of  $\text{Cl}_2$  gas was employed and the Vycor sleeve was omitted. Filter system 5 consisted of Corning CS 7-54 glass filter plates in combination with filter system 3. Filter system 6 was as in filter system 2, except 1.0 g of  $\text{K}_2\text{Cr}_2\text{O}_7$ , 15.4 g of  $\text{K}_2\text{CO}_3$ , and a 200-W Hanovia lamp were employed.

**Analytical Procedures.** NMR, GLC, and UV-visible analytical procedures have been described.<sup>3,17</sup>

**Registry No.** 1,2-A, 83929-15-1; 9,10-A, 83929-13-9; 9,10-dichloroanthracene, 605-48-1.